

Extraction of Transverse Single Spin Asymmetry in J/ψ Production in $p\vec{p}$ Interactions at 120 GeV Beam Energy

Dinupa Nawarathne Dr. Vassili Papavassiliou Dr. Stephen Pate
Forhad Hossain Dr. Abinash Pun

New Mexico State University
Representing the E-1039/SpinQuest Collaboration

New Perspectives 2022
June 16, 2022

FERMILAB-SLIDES-22-050-PPD



- 1 J/ψ Particle
- 2 Transverse Single Spin Asymmetry
- 3 SpinQuest Experiment
- 4 Analysis Procedure
 - Data Generation
 - Gaussian Process Regression (GPR)
 - RooUnfold
- 5 Results and Discussion
- 6 Summary

J/ψ Particle

- J/ψ is a vector meson which is a $c\bar{c}$ bound state.
- Discovered by Burton Richter and Samuel Ting in 1974. Awarded Nobel price for the discovery in 1976.
- In $p\bar{p}$ collisions, J/ψ particles are primarily produced by $q\bar{q}$ annihilation and gg fusion. more details in A. Pun's talk.

$J/\psi(1S)$			
			$J^{PC} = 0^{--}(1^{--})$
Mass $m = 3096.900 \pm 0.006$ MeV			
Full width $\Gamma = 92.9 \pm 2.8$ keV ($S = 1.1$)			
$\Gamma_{ee} = 5.53 \pm 0.10$ keV			
$\Gamma_{ee} < 5.4$ eV, CL = 90%			
$J/\psi(1S)$ DECAY MODES	Fraction (Γ_i/Γ)	Scale factor/ Confidence level (MeV/c)	p
hadrons	$(87.7 \pm 0.5) \%$		—
virtual $\gamma \rightarrow$ hadrons	$(13.50 \pm 0.30) \%$		—
ggg	$(64.1 \pm 1.0) \%$		—
γgg	$(8.8 \pm 1.1) \%$		—
e^+e^-	$(5.971 \pm 0.032) \%$		1548
$e^+e^- \gamma$	[a] $(8.8 \pm 1.4) \times 10^{-3}$		1548
$\mu^+\mu^-$	$(5.961 \pm 0.033) \%$		1545

Figure 2: J/ψ properties. [P. A. Zyla *et al.*, *PTEP* **2020**, 083C01 (2020)]

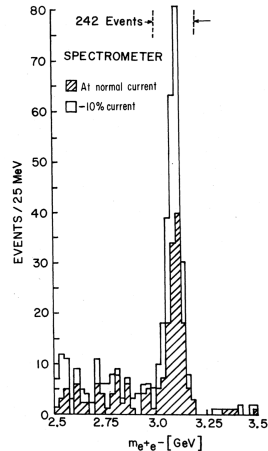


Figure 1: Mass spectrum showing the existence of J/ψ . [J. J. Aubert *et al.*, *Adv. Exp. Phys.* **5**, 128 (1976)]

Transverse Single Spin Asymmetry

- In $p\vec{p}$ collisions, the transverse single spin asymmetry (TSSA), A_N , is defined as the amplitude of the azimuthal angular modulation of the outgoing particle's scattering cross section with respect to the transverse spin direction of the polarized proton.
- The asymmetry can be written as function of azimuthal angle ϕ_S ¹:

$$A(\phi_S) = \frac{N^\uparrow(\phi_S) - N^\downarrow(\phi_S)}{N^\uparrow(\phi_S) + N^\downarrow(\phi_S)} = A_N \sin(\phi_S)$$

- Using this equation we can remove the detector acceptance dependency from the A_N .

¹ ϕ_S is the angle between \vec{S}_{target} and $\vec{p}_{T J/\psi}$.

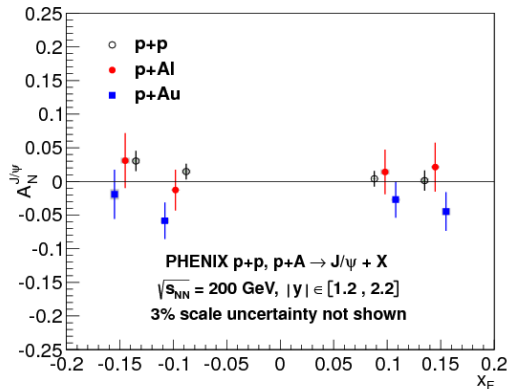


Figure 3: PHENIX results for $A_N^{J/\psi}$ vs. x_F . [C. Aidala *et al.*, *Phys. Rev. D* **98**, 012006, arXiv: 1805.01491 (hep-ex) (2018)]

SpinQuest Experiment

- SpinQuest is a fixed-target Dimuon experiment at Fermilab, using an unpolarized 120 GeV proton beam incident on a polarized solid ammonia target.
- SpinQuest measurements will allow us to test models for the internal transverse momentum and angular momentum structure of the nucleon.
- In the SpinQuest experiment J/ψ production should be dominated by the $q\bar{q}$ annihilation.
- Our goal is to measure A_N with an absolute error $\mathcal{O}(10^{-2})$ for a few p_T and/or x_F bins.
- In this presentation, we demonstrate the analysis procedure and extraction of single spin asymmetry (A_N) for a few p_T and x_F bins.

Anticipated Precision of J/ψ TSSA

Monte-Carlo data

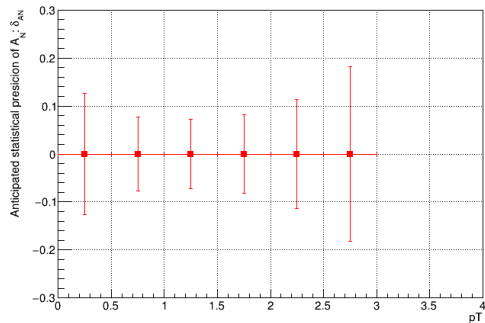


Figure 4: Anticipated Precision of J/ψ TSSA for p_T bins.

Monte-Carlo data

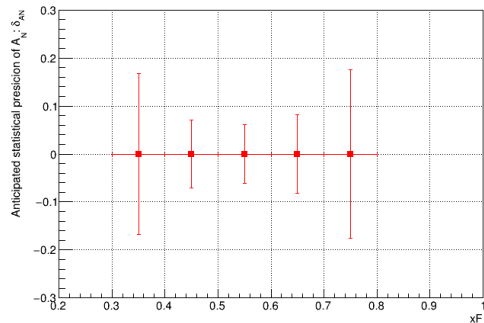


Figure 5: Anticipated Precision of J/ψ TSSA for x_F bins.

■ For one week of dedicated data taking, a precision of ~ 0.1 is expected.

[K. Nakano, DocDB: 9460-v1 (SEAQUEST) (July 2021)]

SpinQuest Experiment

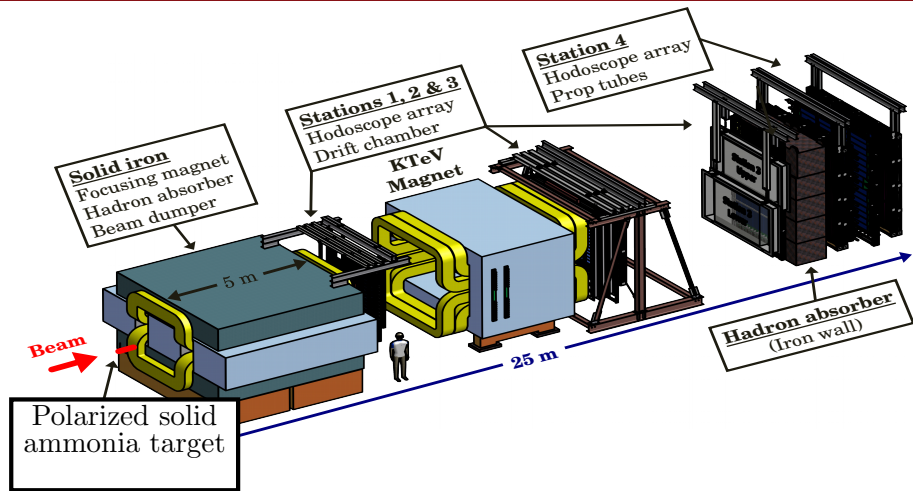


Figure 6: SpinQuest spectrometer. [A. Chen *et al.*, *PoS SPIN2018*, ed. by P. Lenisa *et al.*, 164, arXiv: 1901.09994 (nucl-ex) (2019)]

Data Generation

- Simulated data were generated with kinematics:

- J/ψ events were considered as signal events.

- $x_F = [-0.2, 1.0]$

- where x_F is the the Feynman x.

- Drell-Yan events were considered as background events.

- $x_F = [-0.2, 1.0]$

- $mass = [1.0, 6.0]$

- Asymmetry was introduced by weighting the data ² :

$$w_{A_N} = 1 + A_N \sin(\phi_S - \phi_{\text{phase}})$$

$$w_{\text{Total}} = w_{\text{Gen.}}(mass, x_F) \times w_{A_N}$$

- Asymmetry values are set as $A_N^{J/\psi} = 0.2$ for J/ψ events and $A_N^{BG} = 0.1$ for Drell-Yan events.

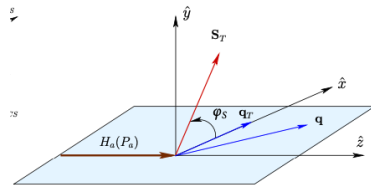


Figure 7: ϕ_S definition in the target rest frame. [R. Longo, *EPJ Web Conf.* **137**, ed. by Y. Foka *et al.*, 05013 (2017)]

² $\phi_{\text{phase}} = 0$. for spin up and $\phi_{\text{phase}} = \pi$ for spin down.

Analysis Procedure

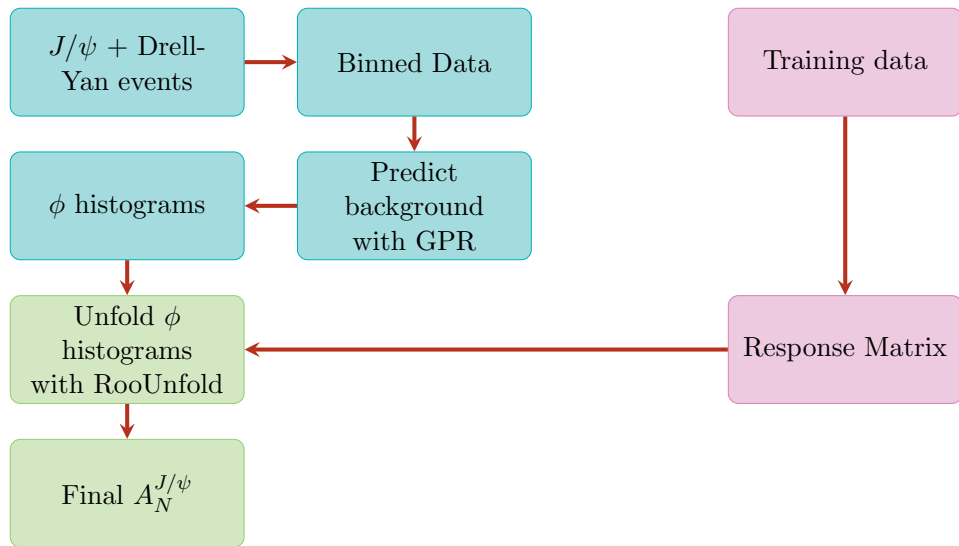


Figure 8: Analysis procedure.

Gaussian Process Regression (GPR)

- Definition: A Gaussian Process is a collection of random variables, any finite number of which have (consistent) joint Gaussian distributions.
- Gaussian processes are distributions over functions $f(x)$ of which the distribution is defined by a mean function $m(x)$ and positive definite covariance function $k(x, x')$, with x the function values and x, x' all possible pairs in the input domain:

$$f(x) \sim \mathcal{GP}(m(x), k(x, x'))$$

where for any finite subset $X = x_1, \dots, x_n$ of the domain of x , the marginal distribution is a multivariate Gaussian distribution:

$$f(X) \sim \mathcal{N}(m(X), k(X, X))$$

with mean vector $\mu = m(X)$ and covariance matrix $\Sigma = k(X, X)$.

Gaussian Process Regression (GPR)

- In this analysis, the Radial-Basis Function (RBF) kernel was used as the kernel function in GPR.

$$k(x_i, x_j) = \exp \left[-\frac{d^2(x_i, x_j)}{2l^2} \right]$$

where l is the length scale of the kernel and $d(\cdot, \cdot)$ is the Euclidean distance.[\[F. Pedregosa et al., the Journal of machine Learning research 12, 2825–2830 \(2011\)\]](#)

- We fit this kernel in side-band regions on either side of the J/ψ invariant mass peak. Then we used the trained kernel to predict the background in the J/ψ peak region.

Predicted Background

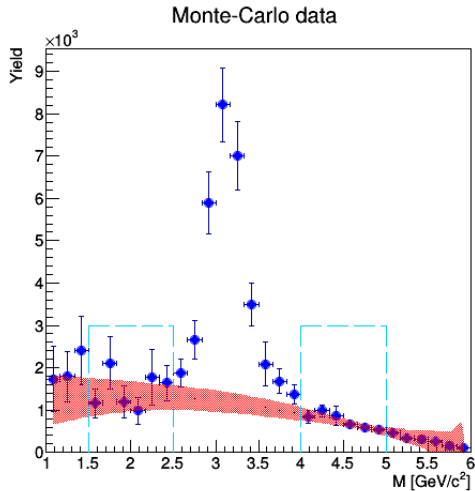


Figure 9: Mass histogram for 1st p_T bin and 1st ϕ bin. Predicted background is given in shaded red region. Side-bands are indicated in dashed blue lines.

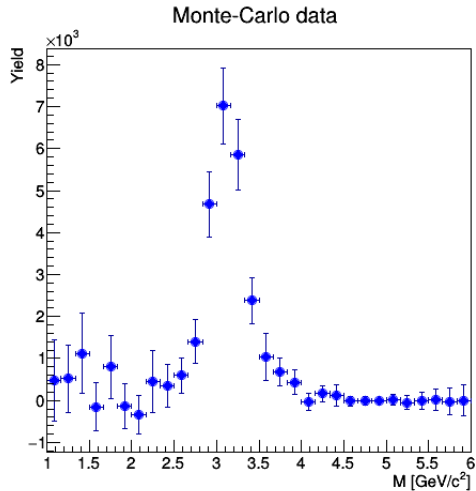


Figure 10: J/ψ signal after subtracting the background.

- Unfolding in high energy physics represents the correction of measured spectra in data for the finite detector efficiency, acceptance, and resolution from the detector to particle level.
- We used the **RooUnfold** package in the analysis. Some default algorithms are:
 - Iterative Bayesian
 - Singular value decomposition
 - Bin-by-bin (simple correction factors)

more details in F. Hossain's talk.

- We trained the response matrix with Drell-Yan events without any asymmetry included.
- We used the iterative Bayesian method to unfold the ϕ distributions. [B. Wynne, [arXiv: 1203.4981 \(physics.data-an\) \(Mar. 2012\)](#)]
- By using the unfolding method we will correct the bin-by-bin migration.

Response Matrix for p_T Bins

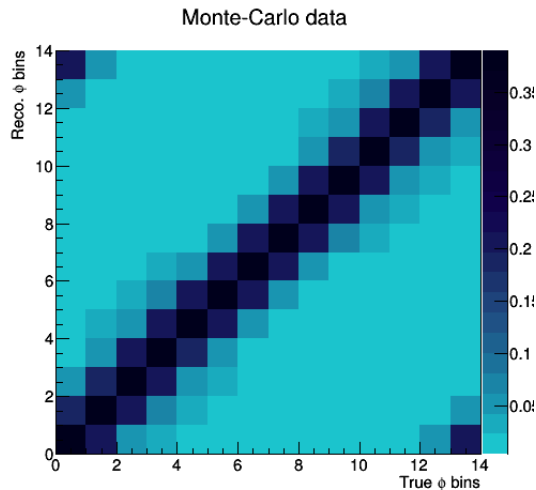


Figure 11: Reco. ϕ vs. true ϕ for $0.0 < p_T < 1.0$.

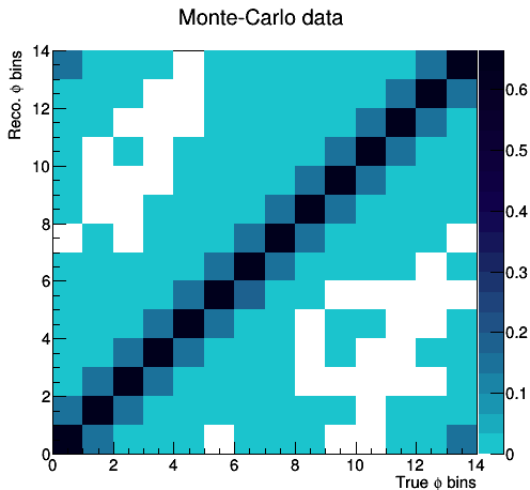


Figure 12: Reco. ϕ vs. true ϕ for $1.0 < p_T < 2.0$.

Response Matrix for x_F Bins

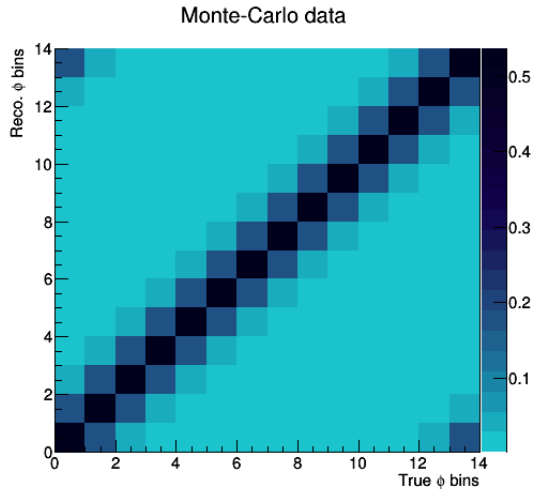


Figure 13: Reco. ϕ vs. true ϕ for $0.4 < x_F < 0.6$.

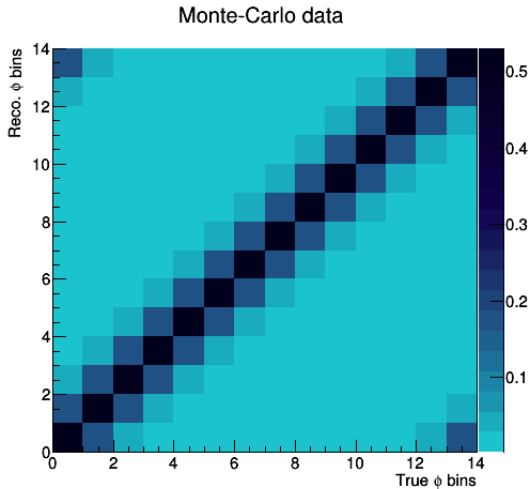


Figure 14: Reco. ϕ vs. true ϕ for $0.6 < x_F < 0.8$.

Unfolded $A_N^{J/\psi}$ in p_T Bins

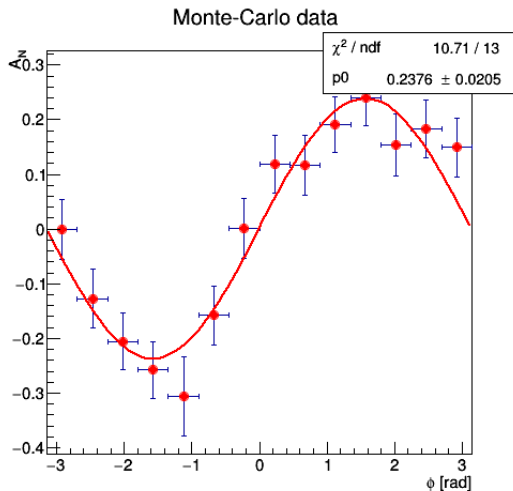


Figure 15: Unfolded asymmetry in $0.0 < p_T < 1.0$.

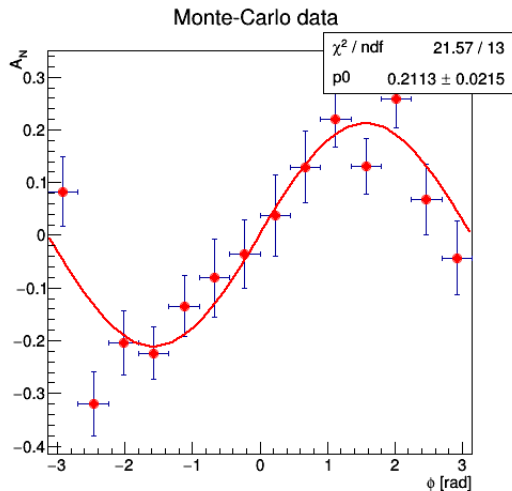


Figure 16: Unfolded asymmetry in $1.0 < p_T < 2.0$.

Unfolded $A_N^{J/\psi}$ in x_F Bins

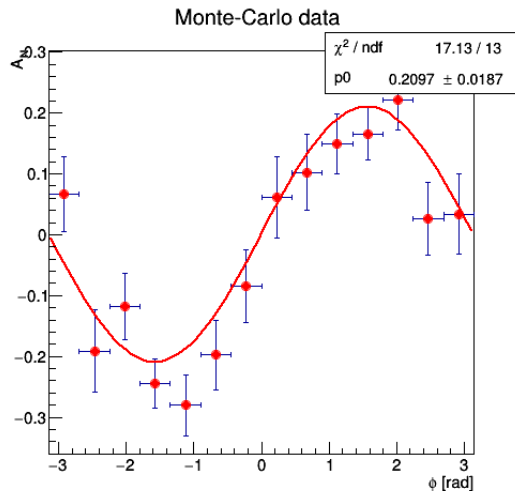


Figure 17: Unfolded asymmetry in $0.4 < x_F < 0.6$.

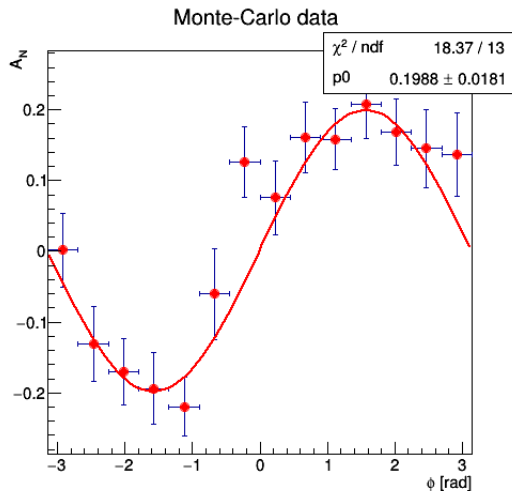


Figure 18: Unfolded asymmetry in $0.6 < x_F < 0.8$.

Extracted A_N

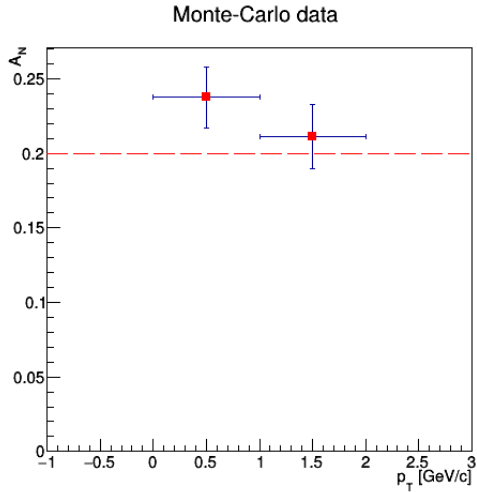


Figure 19: Extracted asymmetry for p_T bins. Generated asymmetry is shown in red dashed line.

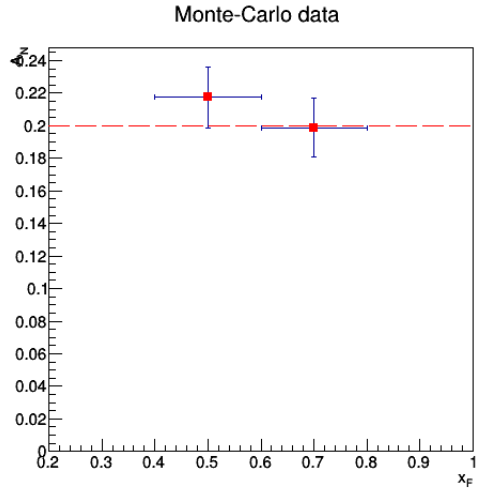


Figure 20: Extracted asymmetry for x_F bins. Generated asymmetry is shown in red dashed line.

Summary

- Gaussian process regression can be used as a good method to predict the background under the J/ψ peak.
- Using iterative Bayesian unfolding, the extracted asymmetry reproduces the generated asymmetry within $1\text{-}\sigma$ confidence interval.
- Installation of the polarized solid ammonia target will be completed at the end of summer 2022 and we expect the 1st beam in fall 2022.
- Acknowledgement:
 - This work is supported by the US Department of Energy, Office of Science, Medium Energy Nuclear Physics Program.

Backup Slides

J/ψ Production

- In $p\bar{p}$ collisions, J/ψ particles are primarily produced by $q\bar{q}$ annihilation and gg fusion.

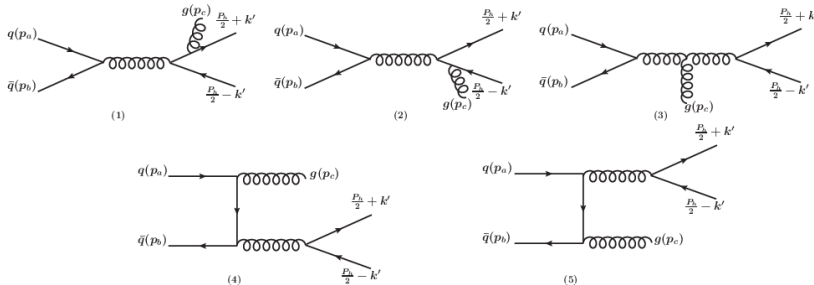


Figure 21: Feynman diagrams for the $q + \bar{q} \rightarrow J/\psi + g$ process. [U. D'Alesio *et al.*, *Phys. Rev. D* **102**, 094011, arXiv: 2007.03353 (hep-ph) (2020)]

J/ψ Production

- In $p\bar{p}$ collisions, J/ψ particles are primarily produced by $q\bar{q}$ annihilation and gg fusion.

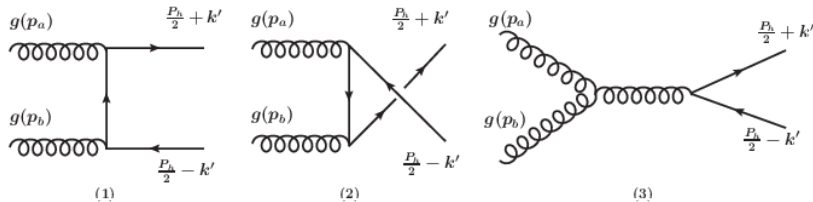


Figure 21: Feynman diagrams for the $g + g \rightarrow J/\psi + g$ process. [U. D'Alesio *et al.*, *Phys. Rev. D* **102**, 094011, arXiv: 2007.03353 (hep-ph) (2020)]

Asymmetry Generation

$$\phi_S = \phi_T + \phi_{\text{phase}}$$

$$\uparrow 1 + A_N \sin \phi_T = 1 + A_N \sin(\phi_S - 0.) = 1 + A_N \sin \phi_S$$

$$\downarrow 1 + A_N \sin \phi_T = 1 + A_N \sin(\phi_S - \pi) = 1 - A_N \sin \phi_S$$

$$A_N(\phi_S) = \frac{N^\uparrow(\phi_S) - N^\downarrow(\phi_S)}{N^\uparrow(\phi_S) + N^\downarrow(\phi_S)} = A_N \frac{2 \sin \phi_S}{2} = A_N \sin \phi_S$$

- The `GaussianProcessRegressor` module in `scikit-learn` was used in this analysis.
- The advantages of Gaussian processes are:
 - The prediction interpolates the observations (at least for regular kernels).
 - The prediction is probabilistic (Gaussian) so that one can compute empirical confidence intervals and decide based on those if one should refit (online fitting, adaptive fitting) the prediction in some region of interest.
 - Versatile: different kernels can be specified. Common kernels are provided, but it is also possible to specify custom kernels.
- The disadvantages of Gaussian processes include:
 - They are not sparse, i.e., they use the whole samples/features information to perform the prediction.
 - They lose efficiency in high dimensional spaces – namely when the number of features exceeds a few dozen.